

Photon Sieve Space Telescope

Geoff Andersen, Mike Dearborn and Geoff McHarg
2354 Fairchild Dr, Ste 2A31
USAF Academy, CO 80840
Contact: geoff.andersen@usafa.edu, 719-333-2829

Introduction

One approach for constructing ultra-large (>20m) next-generation, space-based telescopes is to use membrane primaries. Conventional refractive (lens) or reflective (mirror) elements require perfect three-dimensional surfaces that are impossible to create in zero-g. An alternative is to use a flat diffractive element, which removes the need for out of plane deformation. In this case, the primary is a photon sieve – a diffractive element consisting of millions of holes arranged in circular rings

A Fresnel Zone Plate (FZP) is a diffractive element consisting of concentric transparent and opaque circular zones. The radius (r_n) of the nth bright zone for design wavelength (λ) and focal length (f) is given by:

$$r_n^2 = 2nf\lambda + n^2\lambda^2$$

The requirement of a constant zone area of $\pi\lambda f$ results in a zone width (w) given by:

$$w = \frac{\lambda f}{2r_n}$$

The FZP has the problem that the concentric rings must be supported by some substrate or held in place by supporting ribs. A photon sieve is constructed by centering circular holes of diameter w at the corresponding radial distance r_n . Since there are no connected regions, no transparent substrate or support ribs are required. This permits the construction of a simple structure on a thin reflective membrane.

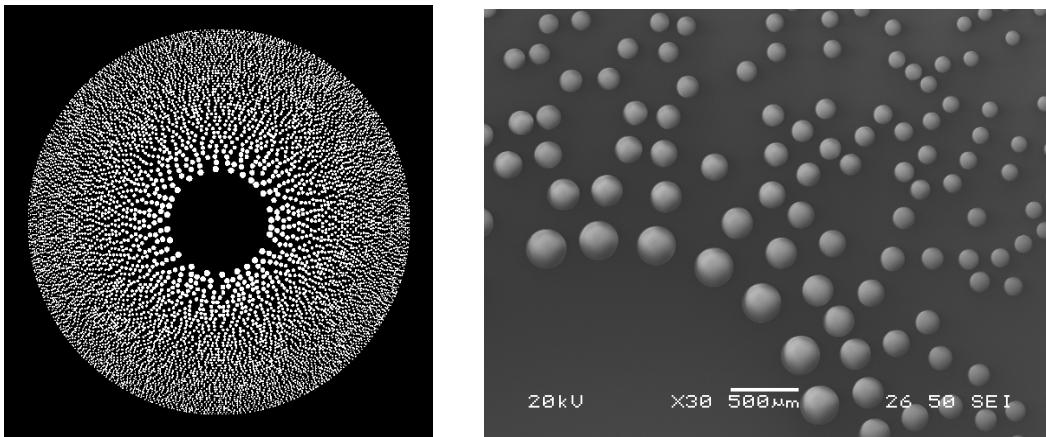


Figure 1: The central section of a photon sieve designed with a random distribution of holes (left) and an SEM photo of one made with holes in chrome coated quartz (right).

Hole Size

More advanced theory has shown that the holes can be made larger than the underlying zone. A hole diameter d can give a positive contribution to the focus so long as the area of overlap with the transparent zone exceeds that of the opaque zone. The magnitude of this contribution is given by:

$$F \propto \frac{d}{w} J_1\left(\frac{\pi d}{2w}\right)$$

where J_1 is the first order Bessel function. The resultant oscillating function is shown below. The first optimum value is for a hole diameter 1.53 times the underlying zone width. Larger ratios (for d/w) are possible, but they rely on higher order diffraction, and reduce the intensity of the final focal spot. For example, it is possible to create an antihole sieve by recentering the holes over dark zones while increasing the hole diameter sufficiently to ensure more transparent zone is obtained than dark zone.

Design and Performance

We have made many different 0.1m diameter photon sieves in chrome-coated quartz patterned by electron beam lithography. In one prototype, we patterned 5 million “antiholes” ranging in size from 10-270 microns diameter (with $d/w=3.514$) to give a sieve focal length of 1m at a wavelength of 532nm. Interferometric analysis (shown below) indicates less than $\lambda/45$ rms error and a Strehl ratio of 0.98. The overall focusing efficiency was 0.3%. The overall field of view was found to be similar to that of a similarly size parabolic mirror.

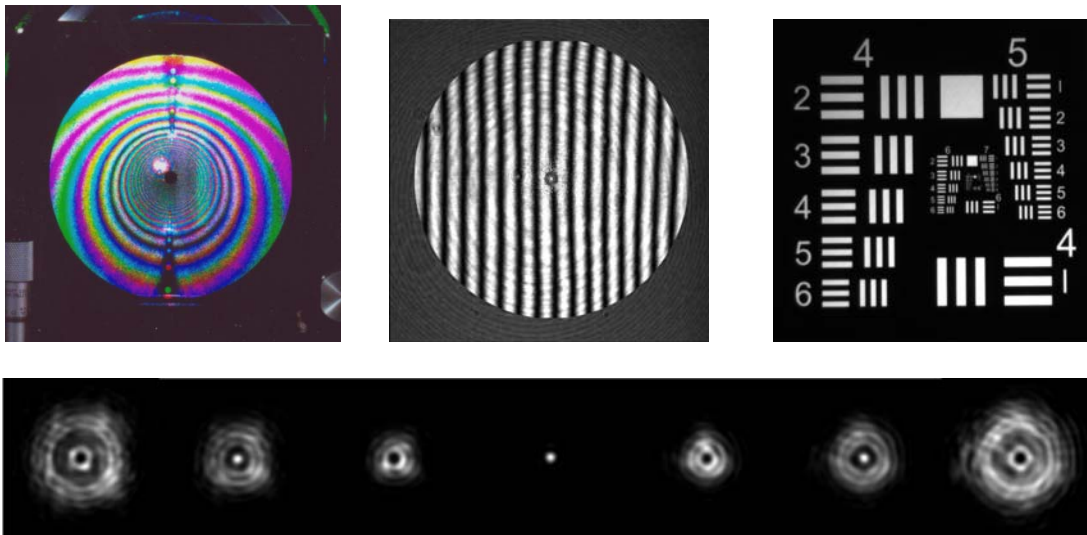


Figure 2: An image of the photon sieve lit by 3 different laser wavelengths (top left), an interferogram of the focused wavefront (top center) and an image produced of a resolution test target (top right). Images of the foci at various axial locations show no spherical aberration (bottom).

Dispersion

Photon sieves, being diffractive elements, suffer from dispersion that results in a focal length varying linearly with wavelength. The depth of focus is thus limited to a bandwidth given by:

$$\Delta\lambda = \frac{2\lambda^2 f}{D^2}$$

We have demonstrated that it is possible to remove a significant amount of this dispersion by using a secondary diffractive element to increase the bandwidth to 40nm or more. As the optic gets faster (smaller f-number) the design constraints on the broadband correction become increasingly and perhaps prohibitively tight. As such the photon sieve is ultimately seen as a high resolution, narrowband imaging option rather than having hyperspectral applications.

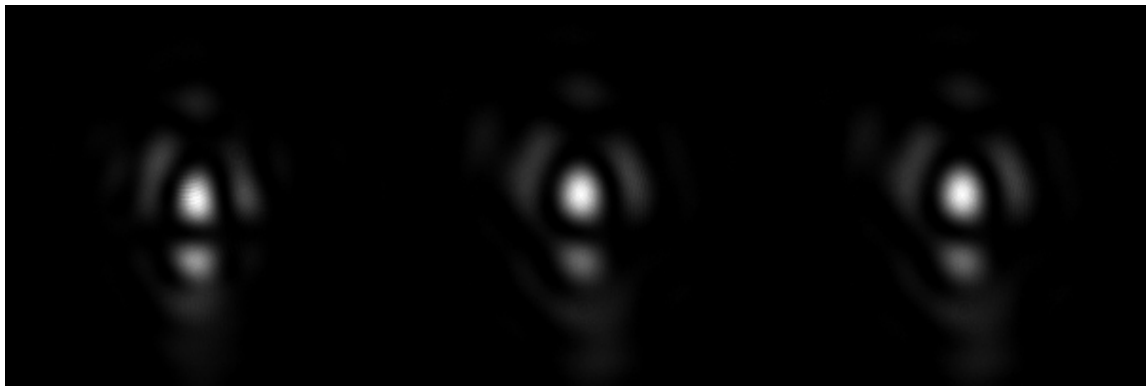
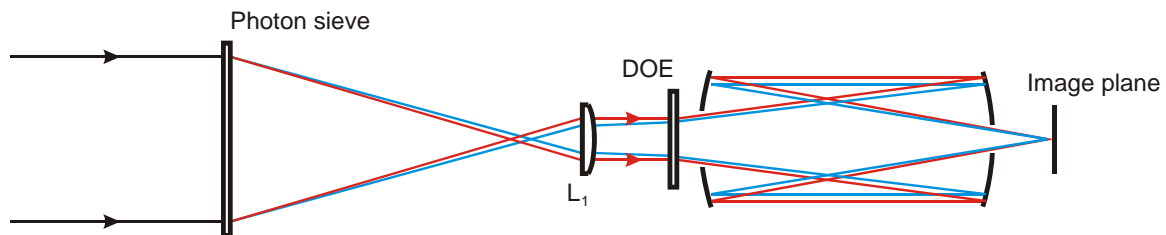


Figure 3: A schematic of the broadband corrected photon sieve telescope (top). Note that the final two mirrors are only used to produce a focus and could in principle be replaced by a single, smaller optic. The resulting experimental demonstration (bottom) shows a constant focal plane for 514nm, 532nm and 543nm light.

Membrane Sieves

Using our successful 0.1m diameter sieves as masters, we created membrane prototypes in 10 micron thick CP1 polyimide coated with aluminum and photoresist. The process involved first creating a glass master and then making a contact print onto the polyimide as shown in the schematic below.

Contact master on to membrane

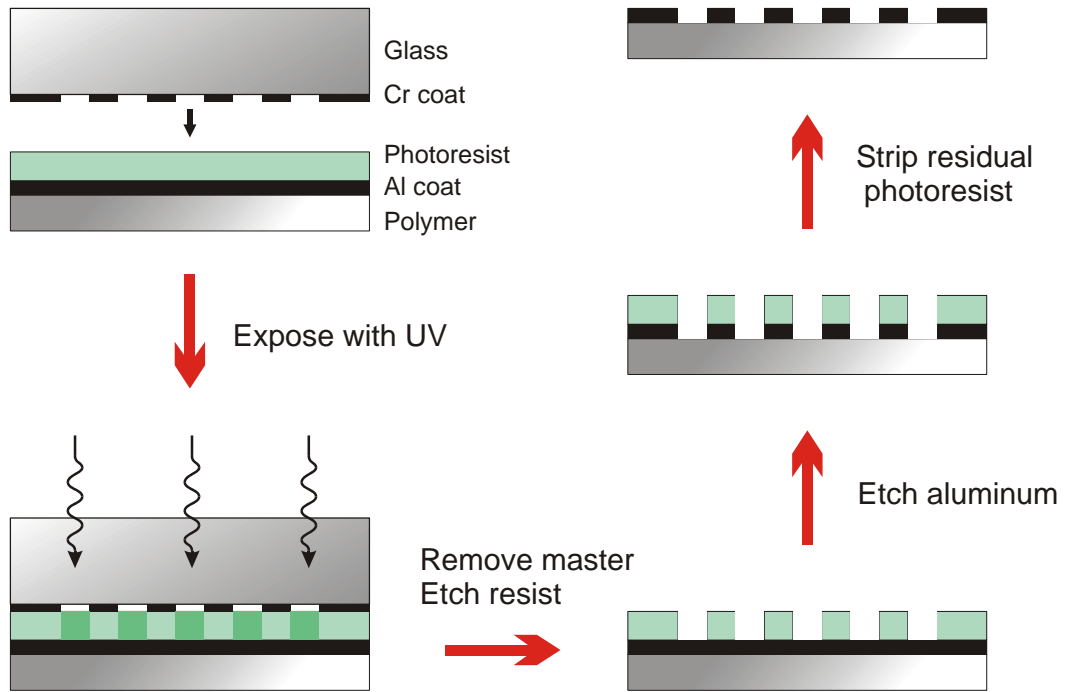


Figure 4: A schematic of the contact print process used to produce an intensity photon sieve on aluminum/photoresist-coated polymer film.

Using our quartz master from the experiments above (Figure 2), we produced transmission photon sieves on CP1 polyimide films bonded to aluminum support rings. Tests showed that the optics performed at the diffraction limit as shown below.

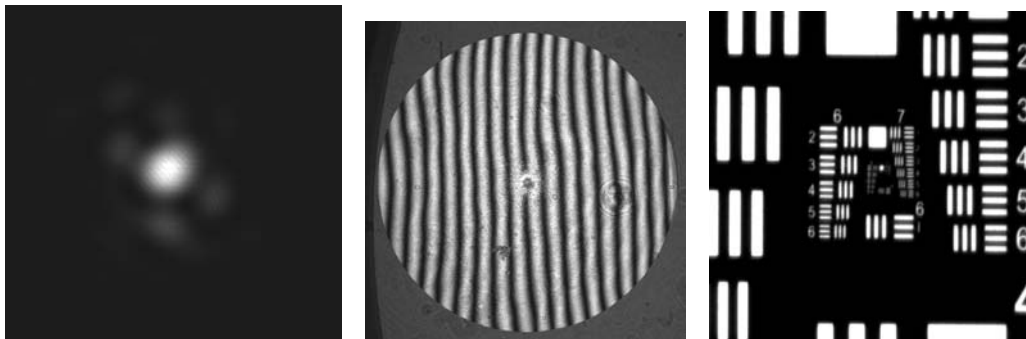


Figure 5: Tests of the membrane photon sieve showing the point spread function (left), interferogram (center) and imaging of a test target (right).

Binary intensity photon sieves produced diffraction limited imaging with 3.5% efficiency. With the fabrication of the aluminum layer thickness to a precise quarter-wavelength height further aluminum coating of the entire substrate can produce exploit phase diffraction for improved efficiency. We produced binary phase photon sieves with an optimum 50% areal fill factor of holes that gave up to 10% efficiency.

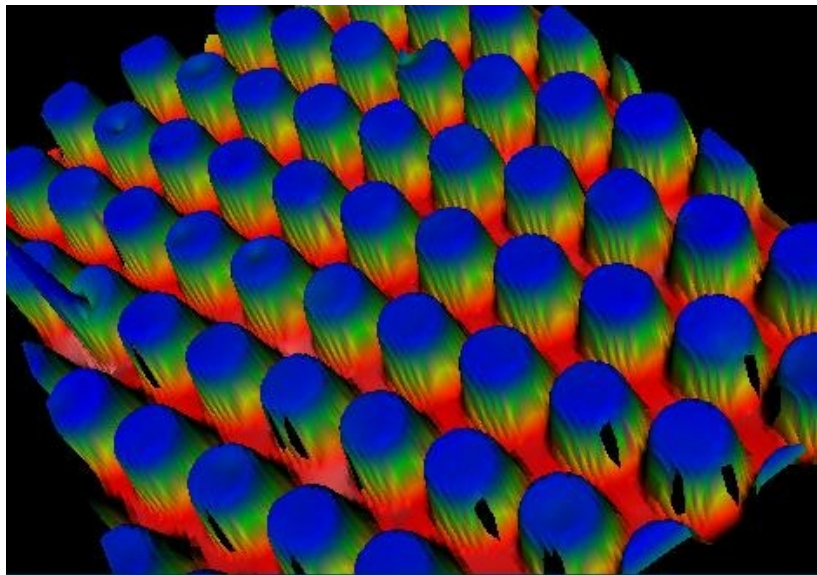
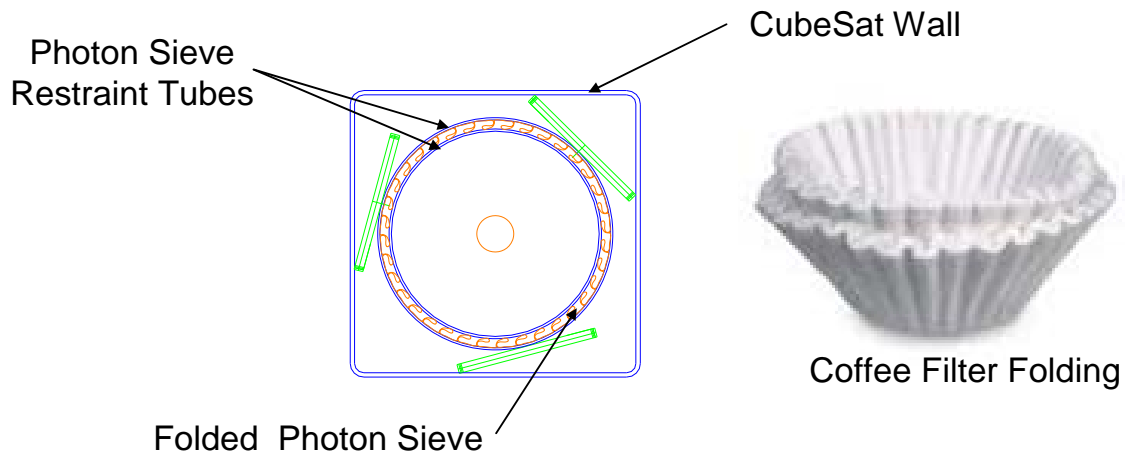


Figure 6: A profilometer was used to measure the structure of the phase photon sieve and shows the circular bumps.

CubeSat Photon Sieve Telescope

We have begun a two-year effort to test and construct a membrane photon sieve for deployment from a 3U CubeSat. With a 0.3m diameter and 1m focal length this element will have around 2.5 billion holes at a wavelength of 656.28nm (H-alpha). Our goal is to test the imaging capability in low Earth orbit using the Sun as a source. The entire sieve, boom structure, imaging optics and camera are configured to stow within just half of the 3U volume available as shown in the images below. Launch is set for 2013.



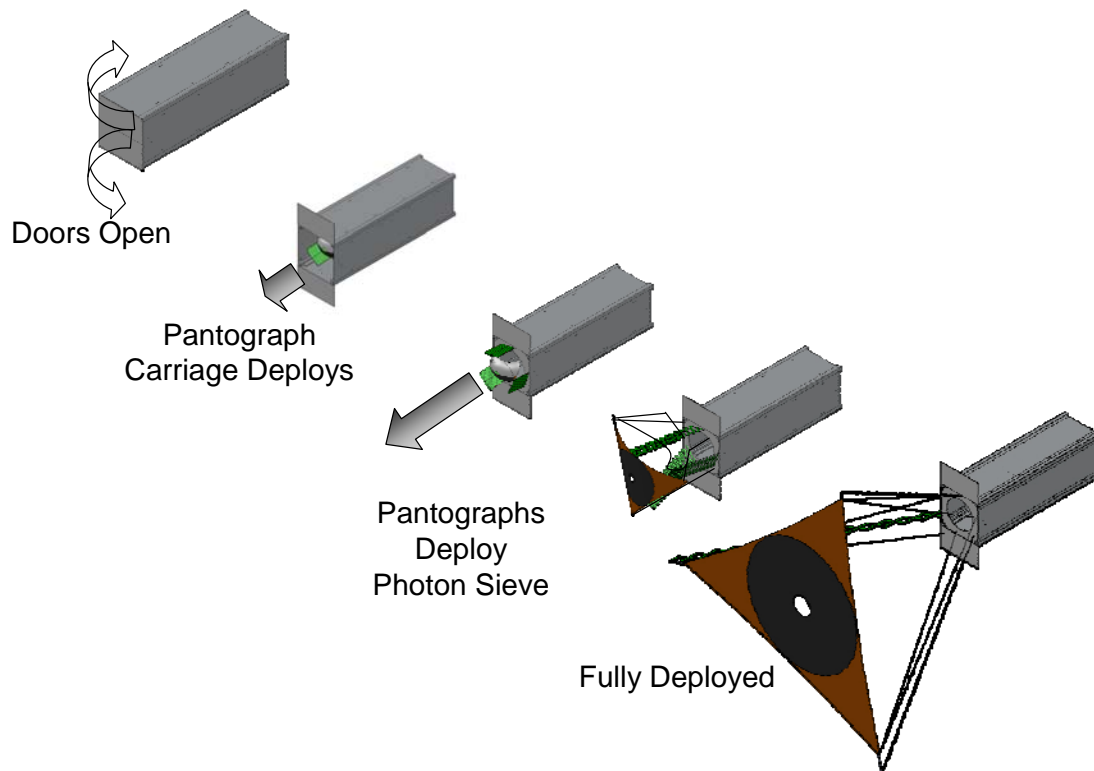


Figure 7: The membrane is to be packed using a “coffee-filter” type arrangement (top). The deployment of the membrane sieve is shown various stages (below).

Acknowledgements

We would like to acknowledge support from the US Air Force Office of Scientific Research (AFOSR), the National Reconnaissance Office (NRO), the US Air Force Research Laboratory (AFRL) as well as Jeff Harvey.

References

1. L. Kipp, M Skibowski, R. L. Johnson, R. Berndt, R. Adelung, S. Harm and R. Seemann, “Sharper images by focusing soft X-rays with photon sieves,” *Nature* 414, 184-188 (2001).
2. Q. Cao and Jürgen Jahns, “Focusing analysis of the pinhole photon sieve: individual far-field model,” *J. Opt. Soc. Am. A* 19, 2387-2393 (2002).
3. Q. Cao and Jürgen Jahns, “Nonparaxial model for the focusing of high-numerical aperture photon sieves,” *J. Opt. Soc. Am. A* 20, 1005-1012 (2003).
4. G. Andersen, “Large optical photon sieve,” *Opt. Lett.* 30, 2976-2978 (2005).
5. G. Andersen and D. Tullson, “Broadband antihole photon sieve telescope,” *Appl. Opt.* 46, 3706-3708 (2007).

6. Zi Lin, Haiyan Wang, Changli Song, Wei Ji, Biao Qi, "Simulation of paraxial pinhole photon sieves model based on Fresnel zone plates," Proc. SPIE 6149, 61493A (2006).
7. Guanxiao Cheng, Tingwen Xing, Yong Yang, Jianling Ma, "Experimental characterization of optical properties of photon sieve," Proc SPIE 6724, 67240D (2007).